Harnessing Vacuum Forces for Quantum Sensing of Graphene Motion

Christine A. Muschik,[1] Simon Moulieras,[1] Adrian Bachtold,[1] Frank H. L. Koppens,[1] Maciej Lewenstein,[1,2] and Darrick E. Chang[1]

[1]*ICFO-Institut de Ciències Fotòniques, Avenida Carl Friedrich Gauss 3, 08860 Castelldefels, Barcelona, Spain*

[2]*ICREA—Institució Catalana de Reçerca i Estudis Avançats, Lluis Companys 23, 08010 Barcelona, Spain*

(Received 4 September 2013; published 3 June 2014)

Position measurements at the quantum level are vital for many applications but also challenging. Typically, methods based on optical phase shifts are used, but these methods are often weak and difficult to apply to many materials. An important example is graphene, which is an excellent mechanical resonator due to its small mass and an outstanding platform for nanotechnologies, but it is largely transparent. Here, we present a novel detection scheme based upon the strong, dispersive vacuum interactions between a graphene sheet and a quantum emitter. In particular, the mechanical displacement causes strong changes in the vacuum-induced shifts of the transition frequency of the emitter, which can be read out via optical fields. We show that this enables strong quantum squeezing of the graphene position on time scales that are short compared to the mechanical period.

DOI: 10.1103/PhysRevLett.112.223601 PACS numbers: 42.50.-p, 42.50.Lc, 34.35.+a, 42.50.Dv

Vacuum forces cause attraction between uncharged objects due to the modification of the zero-point energy in the intervening space [1,2]. They become extremely strong at short distances, which is considered to be a major problem: for example, they lead to stiction and are commonly believed to be "one of the most important reliability problems in micro-electromechanical systems" [3]. However, one can also envision that the strength of vacuum forces enables them to be exploited for applications. A spectacular but challenging example is to engineer repulsive Casimir forces for frictionless devices and levitation [2,4]. Here, we present an application that is possible with current experimental capabilities and without the need to create repulsion.

We describe a technique that enables the highly sensitive displacement detection of a mechanical system [5], which is critical for many devices such as force and mass sensors [6,7]. The ability to sense progressively smaller masses opens up new avenues for studying biological and chemical systems [8–11] and finds exciting applications in surface science [12–14]. A technological push towards faster, high precision measurements would open up the possibility to observe a new class of phenomena, paving the way towards the investigation of molecular diffusion processes and binding at the single molecule level.

Our scheme is based on the Casimir interaction between a surface and a quantum emitter: vacuum fluctuations lead to a modification of electronic state energies, which depends on the presence of nearby surfaces. A moving atom would therefore experience a force associated with the derivative of these shifts [15,16]. A stationary emitter experiences a measurable change in its resonance frequency that depends on the distance to the surface. Finally, if the surface itself moves, such as the suspended nanomechanical membrane in Fig. 1(a), the modulation of the emitter's resonance frequency can be probed, yielding an extremely sensitive displacement detection. This can be done by measuring the phase shift imparted on a field scattered by the emitter [Fig. 1(b)].

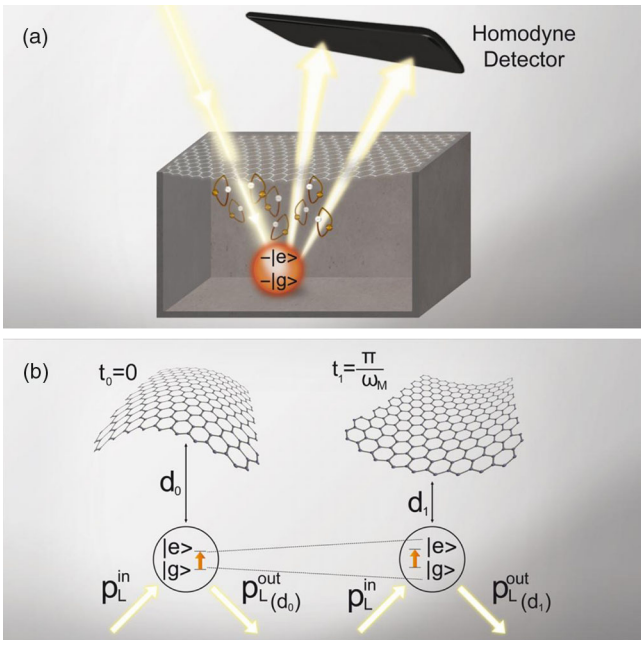

FIG. 1 (color online). Motion sensing via vacuum potentials: (a) A stationary emitter with states $|e\rangle$ and $|g\rangle$ near a suspended graphene sheet is illuminated by a laser. Vacuum fluctuations (illustrated by loops) affect the emitter's transition frequency, while the scattered light is measured by homodyne detection. (b) The membrane and the quantum system interact via vacuum potentials: the emitter's energy levels are shifted depending on its distance d to the membrane. The distance-dependent level shift translates into a phase shift of the light and can be read out by measuring the p quadrature of the scattered field.

There are several major advantages of our approach. First, vacuum interactions between an emitter and a surface are generic to any material. This provides a natural coupling to any mechanical element without the need to additionally functionalize or load it [17–19] or for the material to have low optical losses and high reflection (to integrate with an optomechanical system). Second, vacuum interactions are typically strong and divergent at short scales, providing a strong coupling between the mechanical system and the emitter. We present a general formalism describing the detection of motion based on interactions with a nearby emitter. We describe realistic limits, including backaction, emitter quenching, and imperfect measurement efficiency. We also analyze in detail the case where the mechanical system is a graphene resonator [20–22]. This system is a particularly attractive candidate because its low mass and high Q factor [23] make it promising for a wide class of sensors. However, the capacitive coupling used in state-of-the-art detection techniques [23–25] remains relatively weak. We show that it should be possible to generate a squeezed state of motion in a time that is short compared to the mechanical period, thus approximately achieving the limit of "projective measurement."

The Casimir potential for an emitter in its ground state at position $\mathbf{r}$ can be calculated [15,16] by considering its interaction with the vacuum modes of the electromagnetic field via the dipole Hamiltonian $H_{\rm dip} = -\mathbf{d}\cdot\mathbf{E}(\mathbf{r}) = -\sum_k g_k(\mathbf{r})(|e\rangle\langle g| + |g\rangle\langle e|)(a_k + a_k^\dagger)$, where $\mathbf{d}$ is the dipole moment of the emitter and $\mathbf{E}(\mathbf{r})$ is the electromagnetic field at position $\mathbf{r}$ with normal modes k. We consider a two-level system with states $|g\rangle$ and $|e\rangle$. g_k denotes the vacuum Rabi coupling strength between the emitter and normal mode k with creation operator $a_k^\dagger$ and frequency ω_k. The Casimir shift for an atom in its ground state arises from the nonexcitation preserving terms of $H_{\rm dip}$, which enables the ground state to couple virtually to the excited state and create a photon $|g,0\rangle \to |e,1_k\rangle$, which can be scattered from the surface before it is reabsorbed. The corresponding frequency shift of the ground state due to these fluctuations is given by $\delta\omega_g(\mathbf{r}) = -\sum_k g_k(\mathbf{r})^2/(\omega_0+\omega_k)$, where ω_0 is the unperturbed resonance frequency of the emitter. The shift can be reexpressed in terms of the classical dyadic electromagnetic Green's function $G(\mathbf{r},\mathbf{r},iu)$ evaluated at imaginary frequencies $\omega = iu$,

$$\delta\omega_g(\mathbf{r}) = \frac{3c\Gamma_0}{\omega_0^2}\int_0^\infty du\,\frac{u^2}{\omega_0^2+u^2}\,\mathrm{Tr}\{G(\mathbf{r},\mathbf{r},iu)\}, \quad (1)$$

where c is the speed of light and Γ_0 is the free-space emission rate of the excited state. Similar calculations allow one to determine the excited-state shift $\delta\omega_e$ and modified emission rate $\Gamma(\mathbf{r})$ near the surface [26,27]. At distances d much closer than the free-space resonant wavelength λ_0, the shift in the transition frequency of the emitter typically scales like $\Delta\omega = \delta\omega_e - \delta\omega_g \propto \Gamma_0/(dk_0)^3$ for a bulk material and like $\Delta\omega \propto \Gamma_0\alpha/(dk_0)^4$ for graphene, where α is the fine structure constant and $k_0 = 2\pi/\lambda_0$.

Here, we derive the sensing capability of a single mode of a mechanical system with a single emitter. Regardless of its complexity, any mechanical system can generally be decomposed into a set of normal modes with effective motional mass m, frequency ω_M, displacement x_M, and momentum p_M [28] and a free Hamiltonian of any given mode

$$H_M = \frac{p_M^2}{2m} + \frac{1}{2}m\omega_M^2 x_M^2. \quad (2)$$

As previously described, the displacement of the mechanical system induces a position-dependent level shift on the emitter of the form $H = \hbar\omega(x_M)\sigma_z$, where $\sigma_z = |e\rangle\langle e| - |g\rangle\langle g|$. As we are primarily interested in detecting small displacements, it is suitable to linearize

$$H_{\rm int} = \hbar\omega(x_M)\sigma_z = \hbar g x_M \sigma_z + O(x_M^2).$$

The coupling coefficient $g = (\partial\Delta\omega/\partial x_M)$ describes the rate of change of the emitter frequency per unit displacement.

Next, we provide a quantum description of the emitter interacting with an external laser which probes the emitter's changing resonance frequency. This description consists of two parts: the dynamics of the emitter due to the incoming field and the information about the emitter that is written onto the scattered light. For the former, we restrict ourselves to the interaction with a laser field with Rabi frequency Ω and detuning Δ from the atomic transition at $x_M = 0$, with Hamiltonian $H_{\rm emitter} = (\Delta/2)(|e\rangle\langle e| - |g\rangle\langle g|) + (\Omega/2)(|e\rangle\langle g| + |g\rangle\langle e|)$. The latter is described by $a_L^{\rm out} = -a_L^{\rm in} + \sqrt{\nu\Gamma}|g\rangle\langle e|$, which relates the scattered fields to the atomic coherence. ν characterizes the detection efficiency, Γ is the emitter's total (surface-modified) emission rate, and $a^{\rm in(out)}$ is the annihilation operator of the light before (after) the interaction.

We consider the weak-driving limit, where the population of the atomic excited state is negligible. This limit is characterized by $\epsilon = \Omega^2/(\Gamma^2/4 + \Delta^2) \ll 1$. Physically, working in the limit of $\epsilon \ll 1$ enables the emitter's dynamics to be linearized and ensures that the optical scattering is predominantly coherent. Adiabatic elimination of the emitter yields an emitter-mediated interaction between the membrane and the light. The latter is described by its quadratures $x_L = (a_L + a_L^\dagger)/\sqrt{2}$, $p_L = -i(a_L - a_L^\dagger)/\sqrt{2}$. As explained in the Supplemental Material [29], the reduced system evolves under the Hamiltonian $H = H_M + H_{ML}$, which contains a part describing free motion (M) [see Eq. (2)] and a part describing the interaction between motion and light (ML):

$$H_{ML} = \hbar\kappa x_M p_L. \quad (3)$$

The coupling constant κ reflects the rate at which information about x_M can be obtained and depends on the excited-state population, coupling strength g, and detection efficiency ν. It is given by $\kappa = 2\bar{g}\sqrt{\epsilon\nu/\Gamma}$, where $\bar{g} = g\sqrt{2}(1-(3/8)\epsilon)$ is a renormalized coupling coefficient. In the case of ideal detection efficiency, the rate at which information about x_M [in vacuum units $x_{\rm ZPM} = \sqrt{\hbar/(m\omega_M)}$] can be collected is given by

$\kappa^2_{\text{ideal}} = (4\epsilon\bar{g}^2/\Gamma)$. Since we aim at measuring the mechanical motion on time scales which are short compared to ω_M^{-1}, the dimensionless quantity $(\kappa^2_{\text{ideal}} x^2_{\text{ZPM}}/\omega_M) = (4\epsilon(\bar{g}x_{\text{ZPM}})^2/\Gamma\omega_M)$ represents an important figure of merit characterizing the measurement strength.

The working principle of the scheme can be understood by considering the dynamics in the absence of undesired processes (which will be addressed below) during a short measurement time window $\Delta t \ll \omega_M^{-1}$. In this case, H_{ML} leads to an evolution

$$x_L^{\text{out}} = x_L^{\text{in}} + \kappa\sqrt{\Delta t}\, x_M^{\text{in}}, \tag{4}$$

where the superscripts "in" and "out" denote operators before and after the interaction. For large $\kappa\sqrt{\Delta t}$, all motional properties are mapped onto the output field. Equation (3) also implies that the light imparts backaction onto the membrane $p_M^{\text{out}} = p_M^{\text{in}} + \kappa\sqrt{\Delta t} x_L^{\text{in}}$, which affects the measurement precision for longer times $\Delta t > \omega_M$.

While our analysis thus far was completely general, we now consider the case of graphene [30–37], which has two complicating features. First, its "refractive index" (or, more specifically, its conductivity) can be electrostatically tuned, which alters the level shifts through the Green's function in Eq. (1). Second, graphene can strongly "quench" or absorb light scattered by the emitter, yielding a fundamental upper limit on the detection efficiency ν. Here, we briefly summarize how these properties affect the overall sensitivity of our scheme (see the Supplemental Material [29] for details). Unlike in typical metals, the Fermi energy μ and associated conductivity $\sigma(\omega)$ [38] can be greatly tuned in graphene by applying a voltage [20] or by chemical doping and intercalation [39]. The conductivity directly influences how a proximal emitter interacts with the graphene, leading to three different regimes, as illustrated in Fig. 2. In the first regime of low Fermi level $\mu < 0.5\hbar\omega_0$, the conductivity is mostly real. Graphene is absorptive, as light can induce interband electronic transitions. The total emission rate of the emitter $\Gamma = \Gamma_{\text{rad}} + \Gamma_{\text{nonrad}}$ separates into radiative (i.e., free-space) and absorptive channels, with the latter dominating at close distances. Significant level shifts are observable but with decreased free-space fluorescence [Fig. 2(b)]. The second regime of intermediate Fermi level yields optimal readout sensitivity, as interband absorption becomes suppressed, leading to a sharp decrease in $\text{Re}\sigma(\omega)$, while the level shift is maximum [Fig. 2(c)]. In the third regime of high Fermi level $\mu \gtrsim 0.6\hbar\omega_0$, $\sigma(\omega)$ becomes mostly imaginary and positive, analogous to a thin conducting film. Such thin films support highly localized guided surface plasmons. The emitter can efficiently couple to these modes, which are dark to free-space detection channels and again result in a large Γ_{nonrad} [40–42].

The implications can be seen in Fig. 3(a), where we plot the sensitivity κ^{-1} versus μ and the distance d. Nonradiative emission affects the sensitivity of our scheme since the detection rate κ^2 is proportional to the maximum possible detection efficiency ν. In particular, $\nu = \eta_{\text{det}}(\Gamma_{\text{rad}}/\Gamma)$ contains one term η_{det} describing the efficiency at which photons scattered in free space can be collected and is

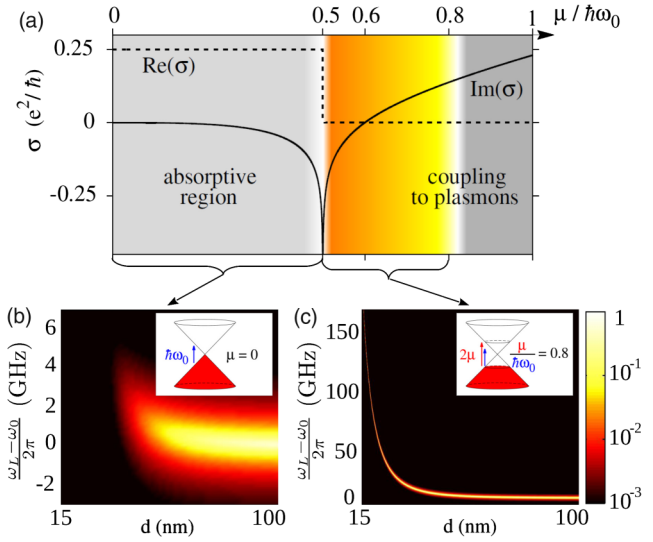

FIG. 2 (color online). Optical properties of graphene and frequency shifts on a nearby emitter: (a) Conductivity σ of graphene versus Fermi energy μ in units of $\hbar\omega_0$, where ω_0 is the emitter's resonance frequency. The real part of the conductivity (dashed line) describes absorption. For $(\mu/\hbar\omega_0) < 0.5$, light radiated by the emitter is absorbed since photons with frequency $\hbar\omega \geq 2\mu$ can induce interband transitions. For $\mu/\hbar\omega_0 > 0.6$, $\text{Im}\sigma > 0$. This implies that the emitter can couple to surface plasmons, which increases its nonradiative decay rate. (b),(c) Radiative photon scattering rate for low excitation power $f(d,\omega_L) = (\Gamma_{\text{rad}}\Omega^2/4)/(\Gamma^2/4 + (\omega_0 + \Delta\omega - \omega_L)^2)$, normalized by the free-space resonant rate $f_0 = \Omega^2/\Gamma_0$ for (b) $\mu = 0$ and (c) $\mu = 0.8\hbar\omega_0$. The shift (broadening) of the peak versus distance reflects the emitter's frequency shift (modified emission rate), while the decrease in contrast reflects increasing emission probability into nonradiative channels.

technical in nature. The other term $\Gamma_{\text{rad}}/\Gamma$ describes the probability for a photon to be scattered to free space (versus absorbed by the material). At an operating distance of $d = 18$ nm, the ideal Fermi level is $\mu = 0.8$. As a concrete example, we consider here $\epsilon = 0.3$, $\eta_{\text{det}} = 0.75$, $\Gamma_0 = 2\pi \times 240$ MHz, and $\lambda_0 = 2 \times 10^{-6}$ m and a graphene sheet with resonance frequency $\omega_M = 2\pi \times 1$ MHz and mass $m = 2.81 \times 10^{-18}$ kg. For these parameters, $\Gamma_{\text{rad}}/\Gamma = 0.54$. The frequency shift per unit length is $g = 2\pi \times 16$ GHz/nm [Fig. 3(b)], which compares very favorably to the best demonstrated couplings in cavity optomechanics experiments [43] and gives rise to a sensitivity of $\kappa^{-1} = 5.6 \times 10^{-16}$ m/$\sqrt{\text{Hz}}$.

The ability to perform highly sensitive position measurements on time scales that are short compared to ω_M^{-1} allows one to create a squeezed state where the variance of the position of the graphene sheet $V_x = \langle x_M^2\rangle - \langle x_M\rangle^2$ is reduced below its zero-temperature variance $V_x < x^2_{\text{ZPM}}$. This comes at the expense of an increased variance of the momentum V_p in compliance with the Heisenberg uncertainty principle $V_x V_p \geq \hbar^2/4$ [see the inset of Fig. 4(a)]. The rotation in phase space would prevent the squeezing of x_M or p_M, if measurements over several oscillation periods were required. However, since the high coupling strength κ

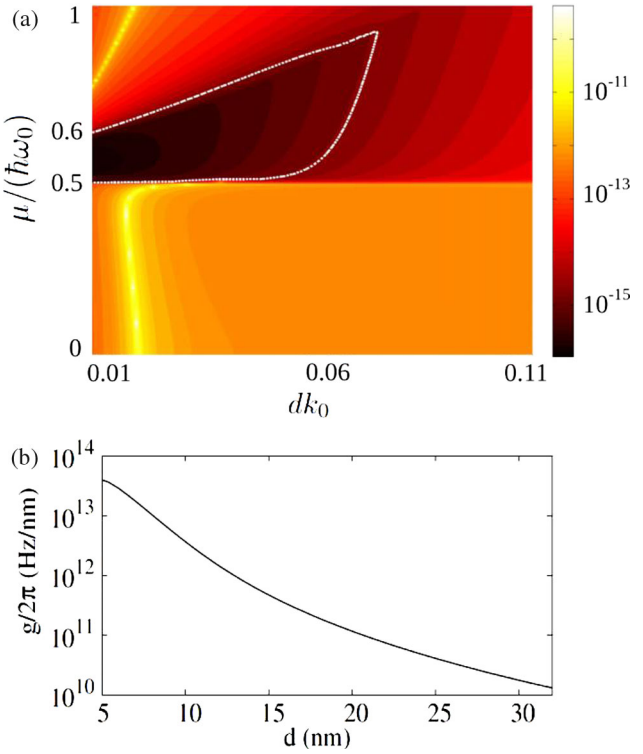

FIG. 3 (color online). Vacuum coupling and detection sensitivity: (a) Inverse coupling strength κ^{-1} in $\mathrm{m}/\sqrt{\mathrm{Hz}}$ versus the distance d and the Fermi energy μ in units of $\hbar\omega_0$, where ω_0 is the emitter's resonance frequency in free space. Within the white line, $\kappa^{-1} < (x_{\mathrm{ZPM}}/\sqrt{\omega_M})$, indicating that measurements at the quantum level are possible with measurement times shorter than the oscillation period. (b) Coupling coefficient $g = (\partial\omega/\partial d)$ in Hz/m versus the distance d in nm for the Fermi energy $\mu = 0.8\hbar\omega_0$ that yields the optimal coupling κ for the considered parameters (see Fig. 4).

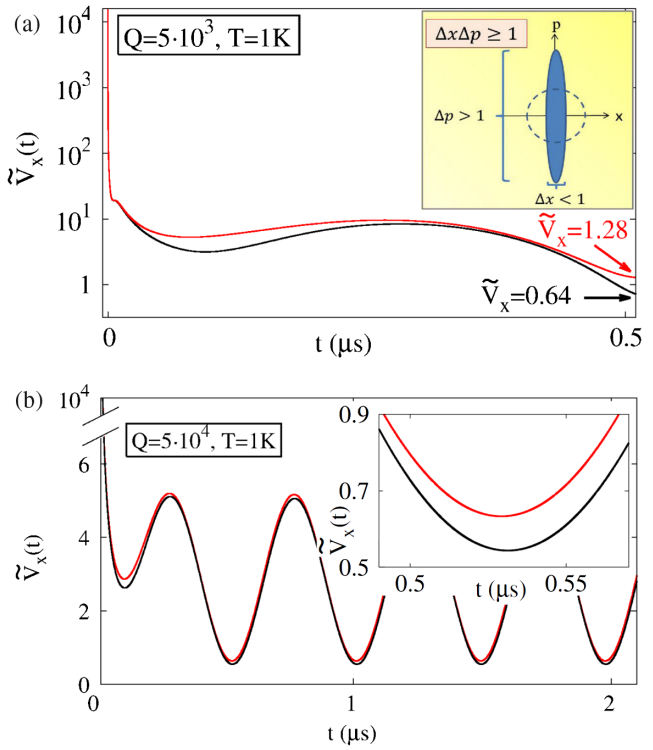

FIG. 4 (color online). Position squeezing of a thermal state at $T = 1$ K: The conditional variance of the position in the rotating frame $\tilde{V}_x(t)$ is shown in units of the zero-point fluctuations x^2_{ZPM} versus time (in μs), (a) during a short time window for $Q = 5 \times 10^3$ and (b) during several oscillation periods for $Q = 5 \times 10^4$. $\tilde{V}_x(t) < 1$ certifies squeezing. Red (black) lines correspond to pure momentum damping $\gamma_x = 0$, $\gamma_p = \gamma$ (symmetric damping $\gamma_x = \gamma_p = \gamma/2$). The used parameters take the values $\omega_M = 2\pi \times 1$ MHz, $m = 2.8 \times 10^{-18}$ kg, $\mu = 0.8\hbar\omega_0$, $d = 18$ nm, $\Gamma_0 = 2\pi \times 240$ MHz, $\lambda_0 = 2 \times 10^{-6}$ m, $\eta_{\mathrm{det}} = 0.75$, and $\epsilon = \Omega^2/(\Gamma^2/4 + \Delta^2)$ (see the main text).

allows for a fast and precise readout, the Casimir scheme yields significant squeezing for realistic Q factors [44], as shown in Fig. 4. Similar results can be obtained for higher temperatures T if the ratio Q/T is kept constant. The ability to perform fast position measurements is interesting for a number of reasons. For example, it can shed light on microscopic origins governing dissipation. As an example, we consider two different damping types: a symmetric model, where position and momentum are damped with equal rates $\gamma_x = \gamma_p = \gamma/2$, and pure momentum damping $\gamma_x = 0, \gamma_p = \gamma$. In the latter case, almost noise-free position measurements can be made in the short time limit, i.e., if the measurement time Δt is short compared to the rotation period in phase space, since momentum damping requires a time span on the order of ω_M^{-1} to affect the position. The high sensitivity of the scheme renders the distinction between different types of damping possible. Symmetric and momentum damping would become indistinguishable if averaged over several oscillation periods but lead to different results if a high temporal resolution is available, as shown in Fig. 4(a). An even greater degree of squeezing can be achieved if the incident light is modulated in time or if short pulses are used [45].

We have shown that quantum vacuum interactions can be a valuable resource for sensing at the quantum level. We have specifically analyzed the scheme for graphene, which is a promising platform for devices but currently lacks the means for fast readout. However, in principle, the presented method is quite general and applicable to a wide class of materials. If the separation between the membrane and the emitter is known, our scheme allows for the precise study and accurate measurement of Casimir forces [46–50], which is an important step towards the vision of controlling and manipulating vacuum potentials. Finally, using specially engineered nanophotonic interfaces could provide even larger dispersive interactions in our scheme, which could lead to the generation of non-Gaussian quantum states of motion.

We gratefully acknowledge discussions with Joel Moser. This work was supported by the ERC Grants QUAGATUA, CARBONLIGHT, CARBONNEMS, and OSYRIS; the

Alexander von Humboldt Foundation; TOQATA (FIS2008-00784); Fundació Privada Cellex Barcelona; the EU Integrated Project SIQS; and the European Commission under Graphene Flagship (Contract No. CNECT-ICT-604391).

[1] H. G. B. Casimir, Proc. K. Ned. Akad. Wet. **51**, 793 (1948).
[2] S. K. Lamoreaux, Rep. Prog. Phys. **68**, 201 (2005).
[3] W. M. van Spengen, R. Puers, and I. De Wolf, J. Micromech. Microeng. **12**, 702 (2002).
[4] J. N. Munday, F. Capasso, and V. A. Parsegian, Nature (London) **457**, 170 (2009).
[5] M. Aspelmeyer, T. J. Kippenberg, and F. Marquardt, arXiv:1303.0733.
[6] J. Moser, J. Güttinger, A. Eichler, M. J. Esplandiu, D. E. Liu, M. I. Dykman, and A. Bachtold, Nat. Nanotechnol. **8**, 493 (2013).
[7] J. Chaste, A. Eichler, J. Moser, G. Ceballos, R. Rurali, and A. Bachtold, Nat. Nanotechnol. **7**, 301 (2012).
[8] T. P. Burg, M. Godin, S. M. Knudsen, W. Shen, G. Carlson, J. S. Foster, K. Babcock, and S. R. Manalis, Nature (London) **446**, 1066 (2007).
[9] A. K. Naik, M. S. Hanay, W. K. Hiebert, X. L. Feng, and M. L. Roukes, Nat. Nanotechnol. **4**, 445 (2009).
[10] M. Li, E. B. Myers, H. X. Tang, S. J. Aldridge, H. C. McCaig, J. J. Whiting, R. J. Simonson, N. S. Lewis, and M. L. Roukes, Nano Lett. **10**, 3899 (2010).
[11] W. H. Grover, A. K. Bryan, M. Diez-Silva, S. Suresh, J. M. Higgins, and S. R. Manalis, Proc. Natl. Acad. Sci. U.S.A. **108**, 10992 (2011).
[12] Z. Wang, J. Wei, P. Morse, J. G. Dash, O. E. Vilches, and D. H. Cobden, Science **327**, 552 (2010).
[13] Y. T. Yang, C. Callegari, X. L. Feng, and M. L. Roukes, Nano Lett. **11**, 1753 (2011).
[14] J. Atalaya, A. Isacsson, and M. I. Dykman, Phys. Rev. Lett. **106**, 227202 (2011).
[15] S. Y. Buhmann, L. Knöll, D. G. Welsch, and H. T. Dung, Phys. Rev. A **70**, 052117 (2004).
[16] S. Y. Buhmann and D. G. Welsch, Prog. Quantum Electron. **31**, 51 (2007).
[17] O. Arcizet, V. Jacques, A. Siria, P. Poncharal, P. Vincent, and S. Seidelin, Nat. Phys. **7**, 879 (2011).
[18] S. Kolkowitz, A. C. Bleszynski Jayich, Q. P. Unterreithmeier, S. D. Bennett, P. Rabl, J. G. E. Harris, and M. D. Lukin, Science **335**, 1603 (2012).
[19] V. Puller, B. Lounis, and F. Pistolesi, Phys. Rev. Lett. **110**, 125501 (2013).
[20] K. S. Novoselov, A. K. Geim, S. V. Morozov, D. Jiang, Y. Zhang, S. V. Dubonos, I. V. Grigorieva, and A. A. Firsov, Science **306**, 666 (2004).
[21] J. S. Bunch, A. M. van der Zande, S. S. Verbridge, I. W. Frank, D. M. Tanenbaum, J. M. Parpia, H. G. Craighead, and P. L. McEuen, Science **315**, 490 (2007).
[22] C. Chen, S. Rosenblatt, K. I. Bolotin, W. Kalb, P. Kim, I. Kymissis, H. L. Stormer, T. F. Heinz, and J. Hone, Nat. Nanotechnol. **4**, 861 (2009).
[23] A. Eichler, J. Moser, J. Chaste, M. Zdrojek, I. Wilson-Rae, and A. Bachtold, Nat. Nanotechnol. **6**, 339 (2011).
[24] V. Gouttenoire, T. Barois, S. Perisanu, J. L. Leclercq, S. T. Purcell, P. Vincent, and A. Ayari, Small **6**, 1060 (2010).
[25] Y. Xu, C. Chen, V. V. Deshpande, F. A. DiRenno, A. Gondarenko, D. B. Heinz, S. Liu, P. Kim, and J. Hone, Appl. Phys. Lett. **97**, 243111 (2010).
[26] I. Prigogine, S. A. Rice, R. R. Chance, A. Prock, and R. Silbey, *Advances in Chemical Physics*, edited by I. Prigogine and S. A. Rice (Wiley, Hoboken, NJ, 1978), Vol. 37.
[27] J. Schiefele and C. Henkel, Phys. Lett. A **375**, 680 (2011).
[28] A. H. Safavi-Naeini, Ph. D. thesis, California Institute of Technology, 2013.
[29] See Supplemental Material at http://link.aps.org/supplemental/10.1103/PhysRevLett.112.223601 for details of the scheme.
[30] S. Ribeiro and S. Scheel, Phys. Rev. A **88**, 052521 (2013).
[31] S. Ribeiro and S. Scheel, Phys. Rev. A **88**, 042519 (2013).
[32] S. Y. Buhmann, S. Scheel, and J. Babington, Phys. Rev. Lett. **104**, 070404 (2010).
[33] S. A. Ellingsen, S. Y. Buhmann, and S. Scheel, Phys. Rev. A **84**, 060501 (2011).
[34] G. L. Klimchitskaya and V. M. Mostepanenko, Phys. Rev. A **89**, 012516 (2014).
[35] M. Chaichian, G. L. Klimchitskaya, V. M. Mostepanenko, and A. Tureanu, Phys. Rev. A **86**, 012515 (2012).
[36] G. L. Klimchitskaya, U. Mohideen, and V. M. Mostepanenko, J. Phys. A **41**, 432001 (2008).
[37] G. L. Klimchitskaya, E. V. Blagov, and V. M. Mostepanenko, J. Phys. A **41**, 164012 (2008).
[38] T. Stauber, N. M. R. Peres, and A. K. Geim, Phys. Rev. B **78**, 085432 (2008).
[39] I. Khrapach, F. Withers, T. H. Bointon, D. K. Polyushkin, W. L. Barnes, S. Russo, and M. F. Craciun, Adv. Mater. **24**, 2844 (2012).
[40] A. Y. Nikitin, F. Guinea, F. J. García-Vidal, and L. Martín-Moreno, Phys. Rev. B **84**, 195446 (2011).
[41] L. Gaudreau, K. J. Tielrooij, G. E. D. K. Prawiroatmodjo, J. Osmond, F. J. García de Abajo, and F. H. L. Koppens, Nano Lett. **13**, 2030 (2013).
[42] F. H. L. Koppens, D. E. Chang, and F. J. Garcia de Abajo, Nano Lett. **11**, 3370 (2011).
[43] A. H. Safavi-Naeini, T. P. M. Alegre, M. Winger, and O. Painter, Appl. Phys. Lett. **97**, 181106 (2010).
[44] C. Chen, S. Rosenblatt, K. I. Bolotin, W. Kalb, P. Kim, I. Kymissis, H. L. Stormer, T. F. Heinz, and J. Hone, Nat. Nanotechnol. **4**, 861 (2009).
[45] M. R. Vanner, I. Pikovski, G. D. Cole, M. S. Kim, C. Brukner, K. Hammerer, G. J. Milburne, and M. Aspelmeyer, Proc. Natl. Acad. Sci. U.S.A. **108**, 16182 (2011).
[46] C. I. Sukenik, M. G. Boshier, D. Cho, V. Sandoghdar, and E. A. Hinds, Phys. Rev. Lett. **70**, 560 (1993).
[47] A. Landragin, J. Y. Courtois, G. Labeyrie, N. Vansteenkiste, C. I. Westbrook, and A. Aspect, Phys. Rev. Lett. **77**, 1464 (1996).
[48] J. N. Munday and F. Capasso, Phys. Rev. A **75**, 060102(R) (2007).
[49] H. Bender, Ph. W. Courteille, C. Marzok, C. Zimmermann, and S. Slama, Phys. Rev. Lett. **104**, 083201 (2010).
[50] D. J. Alton, N. P. Stern, T. Aoki, H. Lee, E. Ostby, K. J. Vahala, and H. J. Kimble, Nat. Phys. **7**, 159 (2011).